

TRANSIENT CONTACT SHEAR STRESS IN A LAYERED ELASTIC QUARTER SPACE SUBJECTED TO ANTI-PLANE SHEAR LOADS

KAZUMI WATANABE

Department of Mechanical Engineering II, Tohoku University, Sendai, Japan 980

(Received 8 September 1975; revised 30 July 1976)

Abstract—In this paper the transient behaviour of a contact shear stress in a layered elastic quarter space subjected to anti-plane shear loads is investigated. The loads are suddenly applied to upper and side edges of the layer. The effects of the reflected waves, the loaded position and the material properties to the contact shear stress are shown graphically.

NOTATION

W_j	displacement in the direction of z -axis
σ_{xz}, σ_{yz}	non-vanishing components of stress
c_j	SH-wave velocity
μ_j	shear modulus
h	thickness of the layer
\mathcal{P}, P, Q	magnitude of the loads
X	$X = x/h$
τ	$\tau = c_j t/h$
L	$L = l/h$
H	$H = h_1/h$
j	subscripts $j = 1$ stands for the layer and $j = 2$ stands for the quarter space

Recently the study of composite material has attracted attention of scientists because of its increasing application to engineering problems. It is well known that one of the most effective factors upon the response for the stress of composite material is the contact shear stress at the interface and the capacity of it is estimated with the strength of junction. The allowances, after which the interface bond has failed, have been made for the contact shear stress by many researchers [1-3].

Besides, it is also important to know the transient behaviour of the contact shear stress due to an impulsive load. However, there have been a few investigations for the transient response of such elastic body having discontinuous material properties as a model of the composite materials. One of the problems of this type was initiated by Achenbach [4], however, the reflected wave affecting the response was not considered in this study.

Then, in order to investigate the transient response of the contact shear stress due to the reflected wave, a problem of a layered elastic quarter space composed of a semi-infinite layer and a quarter space which have different material properties, respectively, is presented. Hence, the layered space is assumed to be subjected to two impulsive anti-plane shear loads P and Q as shown in Fig. 1. So that the loads are antiplane shear loads only, the resulting response is governed by the well known equations

$$W_j{}_{,xx} + W_j{}_{,yy} = c_j^{-2} W_j{}_{,tt}; \quad j = 1, 2 \quad (1)$$

with the following boundary conditions and initial ones,

$$\begin{aligned} \sigma_{xz1} &= Q\delta(y - h_1)H(t), \quad \sigma_{xz2} = 0; & \text{at } x = 0 \\ \sigma_{yz1} &= P\delta(x - l)H(t); & \text{at } y = 0 \end{aligned} \quad (2)$$

$$\begin{aligned} \sigma_{yz1} &= \sigma_{yz2}, \quad W_1 = W_2; & \text{at } y = 0 \\ W_j &= W_j{}_{,t} = 0; & \text{at } t = 0 \end{aligned} \quad (3)$$

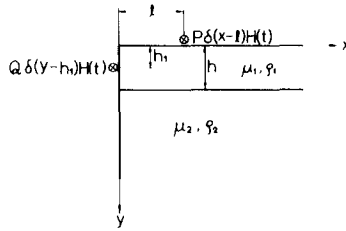


Fig. 1. Coordinates system of the present problem.

where $\delta(\cdot)$ and $H(\cdot)$ are Dirac's delta and Heaviside's unit step functions, respectively, and the repeated subscripts do not mean the summation convention.

The solution of the present problem can be obtained by the method of superposition. In Fig. 2(a) an anti-plane shear load of magnitude \mathcal{P} is placed at $x = l, y = h_1$ in a layer which is located between two half spaces. Using the solution, four solutions of each load located as shown in Fig. 2(b) are easily obtained. Next, superposing the solutions, we can solve the present problem because of symmetry of the loads. That is, since the two loads of magnitude $2P$ are placed at $x = \pm l, y = 0$ and the other two loads of magnitude $2Q$ are at the points of $x = 0, y = \pm h_1$, the normal derivatives of the displacements vanish at $x = 0$ and $y = 0$ except the loaded points and the boundary conditions (2) are also satisfied automatically.

The contact shear stress σ_c at the interface $y = h$ in Fig. 2(a) is easily obtained from reference [5] as

$$\sigma_c = \frac{\mathcal{P}}{2\pi h} F(X, \tau; L, H) \tag{4}$$

where $F(X, \tau; L, H)$ is given in Appendix. Then, the contact shear stress $T_c(X, \tau)$ of the present problem is easily constructed from eqn (4) as

$$T_c(X, \tau) = \frac{P}{\pi h} \{F(X, \tau; L, 0) + F(X, \tau; -L, 0)\} + \frac{Q}{\pi h} \{F(X, \tau; 0, H) + F(X, \tau; 0, -H)\}. \tag{5}$$

It is clear that there are no singularities at the edge point of the interface because of imaging.

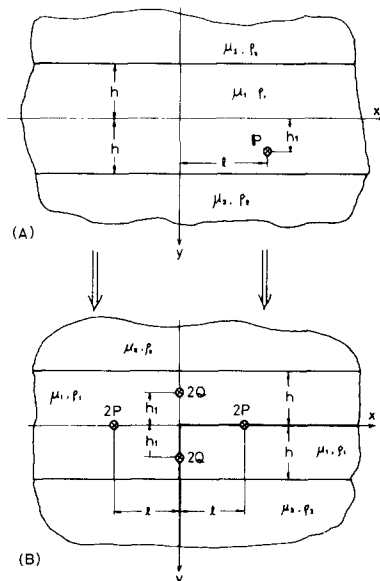


Fig. 2. The schematic construction of the present problem. (a) the single problem; (b) the symmetrically placed four loads problems.

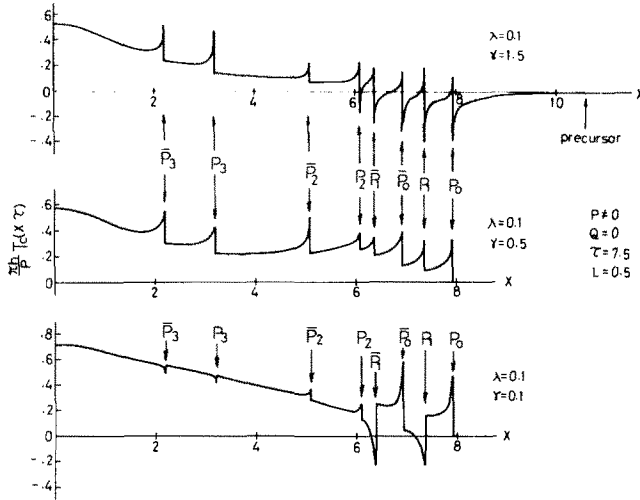


Fig. 3. The variation along the interface of the contact shear stress caused by the upper load P (P_i is the reflected wavefront originated from the loaded point $X = L, Y = 0$ and \bar{P}_i is that originated from the imaging point $X = -L, Y = 0$).

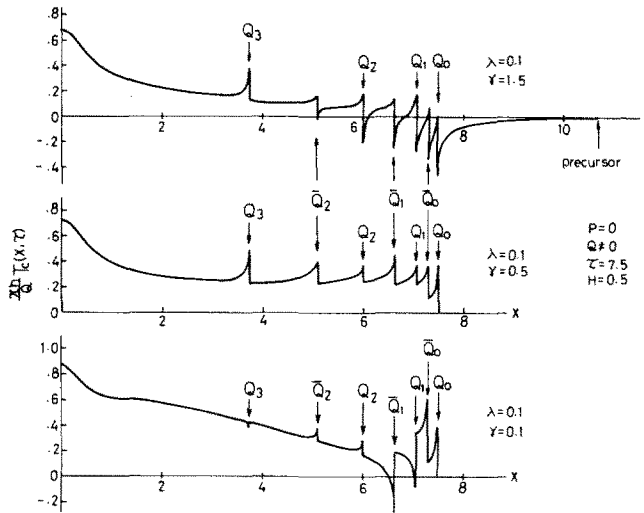


Fig. 4. The variation along the interface of the contact shear stress caused by the side load Q (Q_i is the reflected wavefront originated from the loaded point $X = 0, Y = H$ and \bar{Q}_i is that originated from the imaging point $X = 0, Y = -H$).

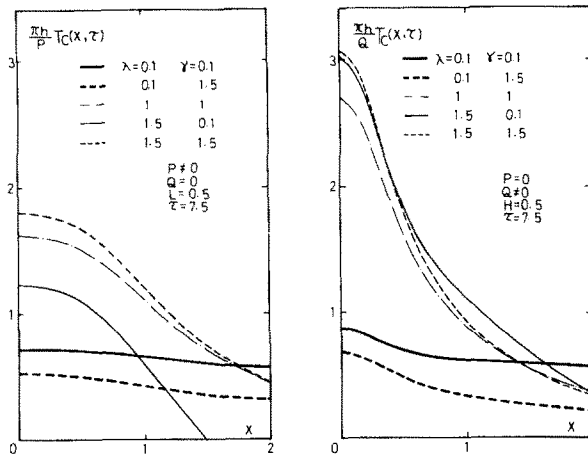


Fig. 5. The variation of the contact shear stress near the edge point of the interface at time $\tau = 7.5$.

However, there are singularities of $O(\Delta\tau^{-1/2})$ at the ordinary reflected wavefronts and of $O(\Delta\tau^{1/2})$ at the reflected fronts of the precursor which only appears in the case $\gamma > 1$.

Numerical calculations are carried out for the case $\lambda < 1$ because the shear modulus of the layer (so-called stiffener) is greater than that of the quarter space (matrix) in general composite materials. Figures 3 and 4 show the distribution of the contact shear stress along the interface at time $\tau = 7.5$ and the reflected wavefronts are denoted by P_n, \bar{P}_n, Q_n and \bar{Q}_n (if $n = 0$, the front is that of unreflected wave). Figure 5 shows the stress near the edge point of the interface.

The following conclusions will be summarized from these results; (a) The multi-reflected wave causes less change in the stress with decrease of the velocity ratio γ , however, the magnitude of the stress is larger in gross sense (Figs. 3 and 4). (b) Near the edge point of the interface the stress is more affected by the shear modulus ratio λ than by the velocity ratio γ and the magnitude of the stress due to the side load Q is larger than that due to the upper load P (see Fig. 5), however, the latter fact is not clear far from the edge point (compare Fig. 3 with 4).

Acknowledgements—The author wishes to express his hearty thanks to Prof. A. Atsumi of Tohoku Univ. for his invaluable directions in the course of the present study and also to Prof. J. D. Achenbach of Northwestern Univ. for his valuable comments. In addition, it should be acknowledged that the expense for the study has been partly appropriated from the Scientific Research Fund of the Ministry of Education for the fiscal year 1976.

REFERENCES

1. V. Laws, P. Lawrence and R. W. Nurse, Reinforcement of brittle matrices by grass fibers. *J. Phys. D.; Appl. Phys.* **6**, 523 (1973).
2. A. Takaku and R. G. C. Arridge, The effect of interfacial radial and shear stress on fiber pull-out in composite materials. *J. Phys. D.; Appl. Phys.* **6**, 2038 (1973).
3. P. Lawrence, Some theoretical considerations of fiber pull-out from an elastic matrix. *J. Mater. Sci.* **7**, 1 (1972).
4. J. D. Achenbach, Transient shear waves in two joined elastic quarter spaces. *J. Appl. Mech.* **36**, 491 (1969).
5. L. Knoppf, Love waves from a line SH-source. *J. Geophys. Res.* **63**, 619 (1958).

APPENDIX

$$F(X, \tau; L, H) = \sum_{n=0}^{\infty} \left[H(\tau - \tau_n) \left\{ T_n(\zeta_n^+) \frac{d\zeta_n^+}{d\tau} - T_n(\zeta_n^-) \frac{d\zeta_n^-}{d\tau} \right\} + H(\bar{X}_n - 1/\gamma) H(\tau - \bar{\tau}_n) H(\tau_n - \tau) \bar{T}_n(\bar{\zeta}_n) \frac{d\bar{\zeta}_n}{d\tau} \right] \quad (A1)$$

where

$$T_n(\zeta) = \frac{\lambda\alpha_2}{\alpha_1 + \lambda\alpha_2} \left(\frac{\alpha_1 - \lambda\alpha_2}{\alpha_1 + \lambda\alpha_2} \right)^n \quad (A2)$$

$$\bar{T}_n(\bar{\zeta}) = \frac{\lambda\bar{\alpha}_2}{\sqrt{\bar{\alpha}_1^2 + \lambda^2\bar{\alpha}_2^2}} \cos \left\{ (2n+1) \tan^{-1} \left(\frac{\lambda\bar{\alpha}_2}{\bar{\alpha}_1} \right) \right\} \quad (A3)$$

$$\zeta_n^* = \{i(X-L)\tau \pm (2n+1-H)\sqrt{\tau^2 - \tau_n^2}\}/\tau_n$$

$$\bar{\zeta}_n = \{\tau|X-L| - (2n+1-H)\sqrt{\tau_n^2 - \tau^2}\}/\tau_n \quad (A4)$$

$$\tau_n = \sqrt{(X-L)^2 + (2n+1-H)^2} \quad (A5)$$

$$\bar{\tau}_n = |X-L|\gamma + (2n+1-H)\sqrt{1-1/\gamma^2} \quad (A6)$$

$$\bar{X}_n = |X-L|/\tau_n \quad (A7)$$

$$\alpha_1 = \sqrt{1+\zeta^2}, \quad \alpha_2 = \sqrt{1/\gamma^2 + \zeta^2}; \quad \text{Re}(\alpha_i) \geq 0 \quad (A8)$$

$$\bar{\alpha}_1 = \sqrt{1-\bar{\zeta}^2}, \quad \bar{\alpha}_2 = \sqrt{\bar{\zeta}^2 - 1/\gamma^2}; \quad 0 < \tan^{-1}(\cdot) < \pi/2 \quad (A9)$$